

Numerical modelling to aid in the structural health monitoring of wave energy converters

William Finnegan^{1,2,a} and Jamie Goggins^{1,2,b}

¹ College of Engineering and Informatics, National University of Ireland, Galway, Ireland

² Ryan Institute for Environmental, Marine and Energy Research, National University of Ireland, Galway, Ireland

^a w.finnegan1@nuigalway.ie, ^b jamie.goggins@nuigalway.ie

Keywords: Irregular linear wave generation; Numerical wave tank; Structural health monitoring; Wave energy converter; Wave-structure interaction.

Abstract. A vital aspect of ensuring the cost effectiveness of wave energy converters (WECs) is being able to monitor their performance remotely through structural health monitoring, as these devices are deployed in very harsh environments in terms of both accessibility and potential damage to the devices. These WECs are monitored through the use of measuring equipment, which are strategically placed on the device. This measured data is then compared to the output of a numerical model of the WEC under the same ocean wave conditions. Any deviations would suggest that there are problems or issues with the WEC. The development of accurate and effective numerical models is necessary to minimise the number of times the visual inspection of a deployed WEC is required. In this paper, a numerical wave tank model is, first, validated by comparing the waves generated to those generated experimentally using the wave flume located at the National University of Ireland, Galway. This model is then extended so it is suitable for generating real ocean waves and a wave record observed at the Atlantic marine energy test site has been replicated in the model to a high level of accuracy. A rectangular floating prism is then introduced into the model in order to explore wave-structure interaction. The dynamic response of the structure is compared to a simple analytical solution and found to be in good agreement.

Introduction

Ocean wave energy is the latest natural resource to be exploited as a renewable source of energy, while also coinciding with the aim of reducing our reliance on non-renewable energy sources. The concept of harnessing ocean wave energy is by no means a new idea. However, the topic only gained international interest in the 1970's with the publication of Stephen Salter's groundbreaking paper on his Wave Energy Duck [1]. One of the main aspects in the design of wave energy converters (WECs) is their survivability and the efficient structural health monitoring (SHM) of these WECs, once they have been deployed into this harsh environment.

The SHM of buildings has been undertaken for decades for both economic and social reasons, including health and safety issues. In 2003, Chang *et al.* [2] published a comprehensive review of the damage detection methods in the SHM of all types of civil infrastructure. In 2004, Guo *et al.* [3] explore the use of improved generic algorithms of SHM to determine the optimum positioning of sensors and the resulting algorithms are then compared to traditional methods. In 2007, Goggins *et al.* [4] used wavelet analysis to develop a SHM algorithm to investigate the seismic response of braced frames. In 2007, Brownjohn [5] details the motivations and reasons for the recent increased interest in the SHM of civil infrastructure and discusses the possible future advances in the area. SHM techniques have also been developed for offshore structures, although not specifically for wave energy converters. For example, in 2003, Nichols [6] experimentally examined the use of low order SHM techniques on two simple models of an articulated offshore structure undergoing ambient excitation. In 2010, Murawski [7] examined measurement and calculation error estimation

Please cite article as: Finnegan W. and Goggins J. (2013). Numerical modelling to aid in the structural health monitoring of wave energy converters. Key Engineering Materials. 569-570: p. 595-602.

DOI: 10.4028/www.scientific.net/KEM.569-570.595 <http://www.scientific.net/KEM.569-570.595>

and damage detection of offshore structures using traditional fibre optics techniques for damaged and undamaged models.

In this paper, numerical models suitable for the modelling of WECs to aid in SHM are discussed and analysed. A numerical wave tank (NWT) is developed using a commercial Reynolds averaged Navier-Stokes equation solver, ANSYS CFX [8], and is based on the methodology, which is described in a previous publication [9]. The model is validated by comparing the waves generated to those generated experimentally using the wave flume located at the National University of Ireland, Galway (NUIG). The model is, then, extended so it is suitable for generating real ocean waves, which are modelling as a linear irregular wave, or a summation of sinusoidal waves. A methodology for generating linear irregular waves has been detailed and a wave record observed at the Atlantic marine energy test site (AMETS) is replicated in the NWT. A rectangular floating prism is then introduced into the model in order to explore the accuracy of wave-structure interaction prediction. A commercial boundary element method software package, ANSYS AQWA [10], is used to perform a hydrodynamic analysis of the structure, in the frequency-domain, and a simple analytical solution, using this analysis, is used to predict the time-domain dynamic response of the structure. This dynamic response and the dynamic response of the structure obtained from the NWT analysis are compared and found to be in good agreement.

Structural health monitoring

In order to perform cost effective SHM of offshore wave energy converters (WECs), it is essential that a reliable and robust remote monitoring system be in place. This system is designed to continuously assess the performance and motions of the WEC in order to automatically highlight or predict structural failures or problems without the need for continuous physical on site inspection, which is very costly and time consuming.

Therefore, the remote SHM system that will be described in this paper will compare the measured output from sensors on the WEC with the output from a NWT model. The NWT model will have the same inputs as the wave conditions over a given time frame, and will, in turn, be comparable to the output from sensors on the WEC. The two sets of outputs will, then, be compared and if the results of comparison are outside a predetermined margin of error, the system will automatically indicate that an on-site visual inspection of the WEC is required.

Consequently, if this system is to operate effectively accurate and robust numerical models, which can accurately mimic real ocean conditions, are required. Furthermore, these models need to accurately perform and predict the wave-structure interaction between the WEC and the real ocean condition. In this paper, NWT models which can accurately replicate real ocean waves and perform wave-structure interaction are described, which are essential if this SHM system is to be successful.

Examples of the type of sensors which can be used to monitor the pressure distribution, or change in force at a point on the structure, are force sensing resistors. These are a polymer thick film device which exhibit a decrease in resistance with an increase in force applied to the active surface. These can also be water proofed so would be ideal for use on a WEC.

Development of an irregular linear NWT

In this section, the methodology for developing a linear NWT, which is described in a previous publication [9], is used to model the NUIG wave flume in order to experimentally validate the accuracy of the methodology. Following on from this validation, the model is extended from linear wave generation to irregular linear wave generation. Since, the aim of the analysis is to replicate a wave record of offshore ocean waves, the wave may be described as an irregular linear wave, which is a summation of linear sinusoidal waves. This model, that can accurately replicate the real ocean wave record, is then used to explore and predict wave-structure interaction at the location of the

record. The structure which is being interacted with in this analysis is a rectangular prism with a unidirectional beam sea incident wave. The dynamic response of the structure, from the CFD NWT analysis, is then compared to a simple analytical solution which is calculated from a frequency domain hydrodynamic analysis of the structure.

Validation of NWT using experimental data. A linear NWT model of the NUIG wave flume, shown in Fig. 1 (b), is used to validate the methodology described in a previous publication [9] by comparing to experimentally generated data. The experimental wave flume located at NUIG is 10m x 1m x 1m with a still water level of 0.7m. A wedged-shaped plunger-type wavemaker is used to generate linear waves with a wave period of 0.75 – 2 seconds. In order to dissipate the wave energy at the end of the flume, there is a beach in place, with a slope of 3:1, and a raised sponge mesh along the SWL for the end 800m. Thus, the tank has an effective length of approximately 7m. There are wave elevation gauges, or probes, in place at 2.35m and 4.75m from the wavemaker which capture the free surface elevation as it varies with time.

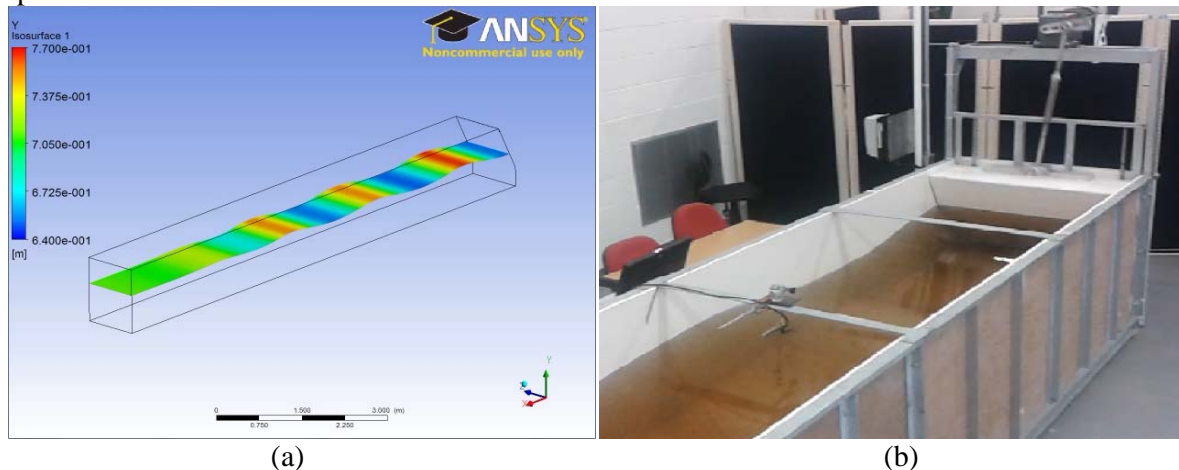


Fig. 1: Linear wave generation using a plunger type wavemaker. (a): CFD NWT model. (b): Experimental wave flume at NUIG.

For the purpose of validating the methodology, the linear NWT model of the NUIG wave flume uses a numerical wedged-shaped plunger-type wavemaker to generate the linear waves, shown in Fig. 1 (a), and the wave elevation is monitored at the same locations along the tank as the wave elevation gauges in the experimental flume. However, the viscosity of the fluid is adapted nearing the end of the model so to dissipate the wave energy, which is described in the next section. This assumes that all the wave energy is dissipated, which is not the case, but it is a more accurate representation than just putting a beach in place which is the other option. The output from the NWT and the experimental observations from the two wave elevation gauges are compared in Fig. 2 and are found to be in good agreement.

Real-time ocean wave record. The measured wave records, which are to be replicated in this analysis, have been recorded at the Atlantic marine energy test site (AMETS) off Belmullet, Co. Mayo Ireland [11] on 02-09-2011 beginning at 17:00. The first 200 seconds of the record can be seen in Fig. 1. AMETS has been selected for the full-scale testing of pre-commercial wave energy devices. The site itself provides facility for the testing of near-shore, intermediate-water and offshore devices and was selected principally due to its deep water with sandy seabed close to shore, the quality of its wave climate, the on shore infrastructure and the suitable grid connection. A Fugro Wavescan buoy is used to record the real-time wave data and is located approximately 3 km offshore in 50-100 m water depth.

Irregular linear NWT model set-up. The model set-up used in this analysis is mainly based on a previous publication [9]. The set-up is divided into three stages: (1) the geometry set-up, which defines the physical dimensions of the model, (2) the mesh set-up, where the computational domain mesh is created and (3) the wave-water, or physics, setup, which defines the analysis type, the

domain setup, the boundary conditions, the initial water height and other characteristics of the water and air-water interaction.

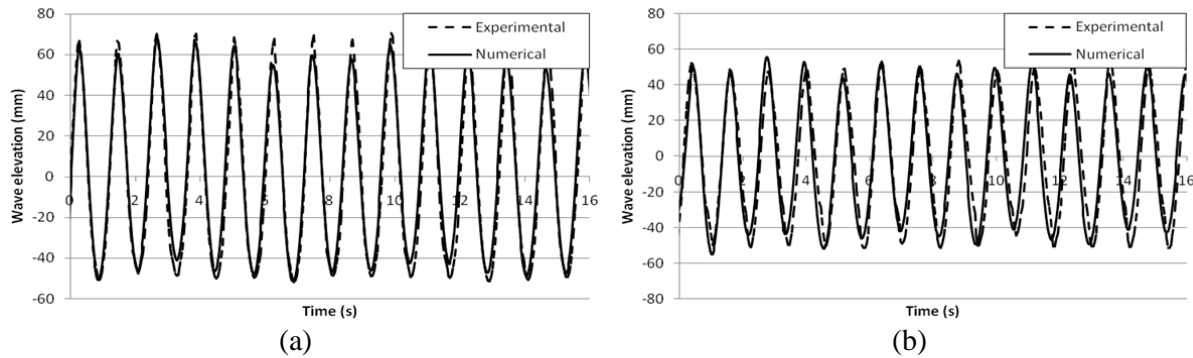


Fig. 2: Comparison between the output from the NWT model and the experimental output from the NUIG wave flume at a distance from the wavemaker: (a) 2.35m and (b) 4.75m

The geometry of the model is rectangular in plan with a thickness less than the size of an element. Two symmetry boundaries will be placed so the NWT is infinitely wide so there is no need to have the model any thicker. There is a limitation in the software license that the maximum dimension is 500m. Therefore, the total length of the model is 500m and total height of 120m, with a still water level (SWL) of 70m.

Since the volume of fraction method is used to define the water level, it is necessary to refine the mesh at the SWL in order to capture the free surface accurately, which is shown in **Error! Reference source not found.** This technique is similar to that employed by Finnegan and Goggins [9], Lal and Elangovan [12] and Liang *et al.* [13]. The thickness of the refined mesh at the SWL is dependent on the maximum amplitude of the wave with a maximum element size of 0.3m. The remainder of the domain has a maximum element size of 3.5m. The total number of elements for the computational domain is approximately 11000 for all simulations described.

In defining the domain set-up, a number of assumptions are included. The surface tension at the air-water interface is assumed to be negligible. From previous studies [9, 12], it was found that the turbulence model used doesn't affect the generated wave. In this analysis a shear stress transport model is used which is also the model used by Elangovan [14]. An initial hydrostatic pressure is specified in the 'Water' region with no pressure in the 'Air' region and the entire region is static initially. The air is specified to a temperature of 25°C and, therefore, its density is specified to be 1.185 kg/m³. Furthermore, an isothermal heat transfer model is specified, which is homogeneous. The fluid (water) temperature is defined as 25°C and its density is given as 997 kg/m³. The viscosity of the water is 8.899 x 10⁻⁴ kg/ms for the first 300 m of the model. Then the viscosity is used to dissipate the energy in the wave, increasing linearly to 125000 kg/ms as it reaches the outflow boundary. Therefore, the viscosity is defined as:

$$\mu = \begin{cases} 8.899 \times 10^{-4}, & x < 300 \text{ m} \\ 8.899 \times 10^{-4} + \frac{x - 300}{200} 125000, & x \geq 300 \text{ m} \end{cases} \quad (1)$$

Instead of using a physical wavemaker, for example the flap-type wavemaker used in Finnegan and Goggins [9], a velocity inflow boundary is used to generate the incident wave. The input wave at the inflow boundary is in the form of an irregular linear wave with corresponding water particle velocities below the water level. The Fast Fourier transform (FFT) of the wave record at AMETS is utilised in order to deduce this irregular linear wave, which is a summation of N sinusoidal waves. Therefore, the wave elevation, $\eta(t)$, being inputted at the inflow boundary is:

$$\eta(t) = \sum_{n=1}^N A_n \cos(-\omega_n t - \varepsilon_n') \quad (2)$$

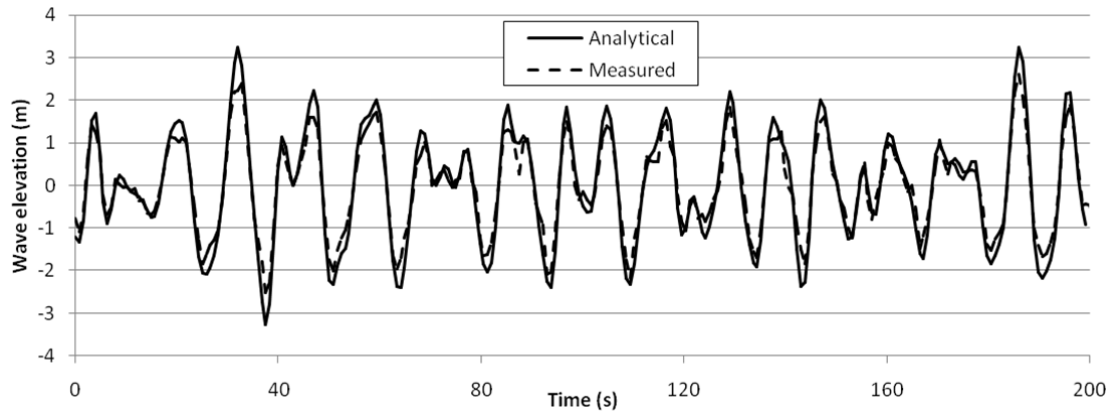


Fig. 3: Comparison between the measured wave at AMETS and the analytical approximation beginning at 17:00 on 02-09-2011

where t is time, A_n is the wave amplitude, ω_n is the wave angular frequency and ε_n' is a function of the FFT phase angle and the distance from the input boundary of the desired wave of the n th linear wave. A comparison between the measured wave and this analytical approximation can be seen in Fig. 3. Similar to the approach of Zhao *et al.*[15], Dong *et al.*[16] and Xu *et al.*[17], the horizontal and vertical water particle velocities, along with the wave elevation given in Eqn. (2), are specified at the input boundary. From linear (Airy) wave theory [18], the water particle velocities are given as:

$$u_1(t) = \sum_{n=1}^N A_n \omega_n \frac{\cosh(k_{0,n} y')}{\sinh(k_{0,n} d)} \cos(-\omega_n t - \varepsilon_n') \quad (3)$$

and

$$u_2(t) = \sum_{n=1}^N A_n \omega_n \frac{\sinh(k_{0,n} y')}{\sinh(k_{0,n} d)} \sin(-\omega_n t - \varepsilon_n') \quad (4)$$

where $u_1(t)$ and $u_2(t)$ are the horizontal and vertical water particle velocities, respectively, and y' is the vertical distance from the base of the model. When entering the water particle velocities at the input boundary, the VOF is utilised to differentiate between the 'Air' and 'Water' regions.

The top of the model has an opening boundary condition, which allows air to pass through. At the inflow boundary, the wave elevation and horizontal and vertical water particle velocities need to be specified. An insignificant initial horizontal air velocity is also specified. The volume of fraction is utilised here to differentiate between the 'Water' velocities and 'Air' velocities. The details of these inputs are described in more detail in the next section and are inputted using the ANSYS CFX expression language (CEL) [8]. At the outflow boundary there is a hydrostatic pressure specified up as far as the initial SWL to allow for overspill of excess water and allow air to pass. There are symmetry boundary conditions specified for the adjacent sides, in order to create a model that is infinitely wide, and the remaining boundaries are assigned a static wall boundary condition.

A comparison between the analytical approximation of the measured wave and the output from the CFD model can be seen in Fig. 4. Since the model starts from a steady state, there is no correlation between the two waves in the initial stages of the simulation. However, after this stage, the two waves are found to be in very good agreement in terms of both frequency and amplitudes.

Irregular linear wave-structure interaction. The next stage of the analysis is to introduce a structure into the model. In this paper, an infinitely long rectangular prism is used as the structure in order to analyse the accuracy of the model's prediction of the dynamic response of a structure in the presence of an irregular linear wave. The infinitely long rectangular prism has a width of 30m, a draft of 15m, with a total structural height of 20m, and its centre is at a distance of 200m from the inflow boundary.

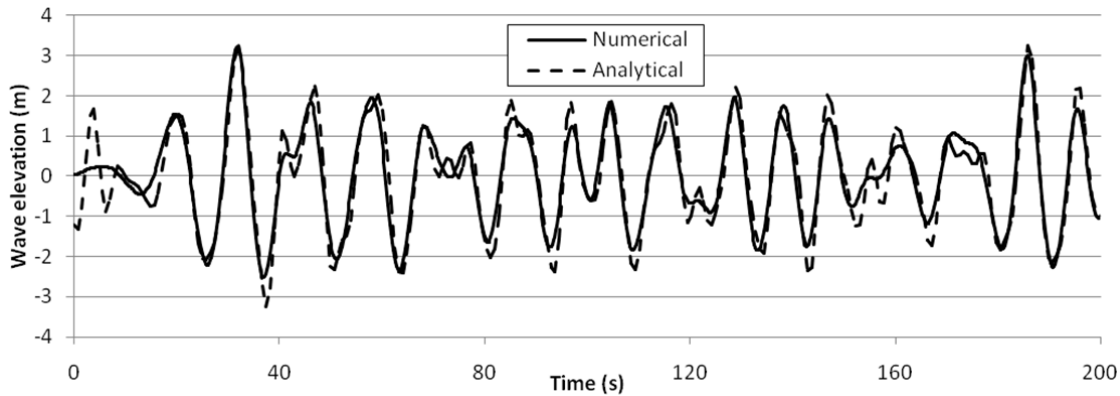


Fig. 4: Comparison between the analytical approximation wave and the output wave from the CFD model beginning at 17:00 on 02-09-2011

The ‘*Rigid Body*’ fluid-structure interaction feature of ANSYS CFX [8] is used to model the structure. This feature requires a number of properties of the structure, including, centre of gravity, moments of inertia, translational and rotational degrees of freedom and either initial velocity or initial acceleration components. In this analysis, the structure is restricted to vertical movement alone, the initial velocity components are zero and its centre of gravity is set equal to its initial centre of buoyancy. It may be noted that when the structure is introduced, additional mesh refinement is required around the structure. The ‘*Sphere of Influence*’ mesh refinement method is used and, therefore, the total number of elements in the mesh is increased to 40000. The linear irregular wave-structure interaction can be seen in Fig. 5 at 142.6 seconds.

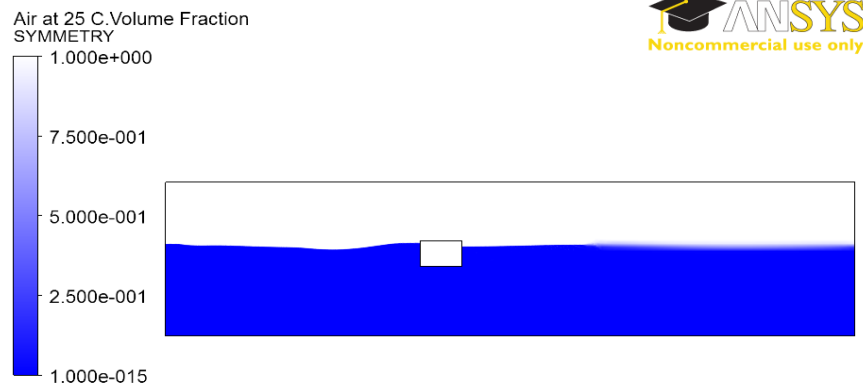


Fig. 5: Wave profile and dynamic response of the structure at 142.6 seconds

Furthermore, so as to assess the accuracy of the model, the dynamic response from the NWT is compared to a simple analytical solution derived from the hydrodynamic analysis of the structure. The hydrodynamic analysis is performed using the commercial boundary element method software package ANSYS AQWA [10]. A parametric study on the length of the prism required to accurately replicate the normalised dynamic response of the infinitely long structure to beam sea conditions and a length of 100m was deemed sufficient. The normalised dynamic response, \hat{u} , and the phase angle, β , is shown graphically in Fig. 6. The dynamic response is determined analytically, u , in the time-domain, using the following expression:

$$u(t) = \sum_{n=1}^N A_n \hat{u}_n \cos(-\omega_n t - \varepsilon'_n - \beta_n) \quad (5)$$

A comparison of the dynamic response of the structure from the NWT model and the analytical solution, given in Eq. (5), is shown in Fig. 7. The two solutions were found to be in good agreement. The two solutions match very well in terms of frequency but there is a difference in the

Citation: Finnegan W. and Goggins J. (2013). Numerical modelling to aid in the structural health monitoring of wave energy converters. Key Engineering Materials. 569-570: p. 595-602.

DOI: 10.4028/www.scientific.net/KEM.569-570.595 <http://www.scientific.net/KEM.569-570.595>

amplitude of the response. This may be attributed to; in the NWT model the structure is restricted to heave, or vertical, motion only while in the hydrodynamic analysis, all degree of freedom are accounted for.

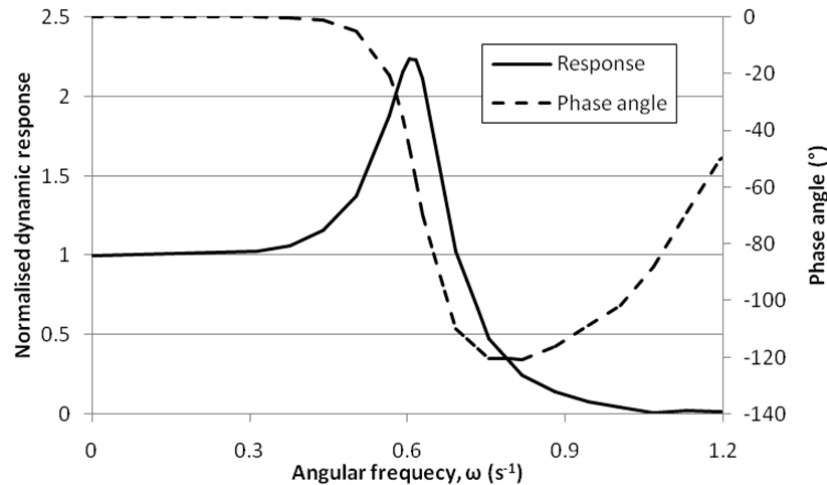


Fig. 6: The normalised dynamic response and associated phase angle from the hydrodynamic analysis of the structure

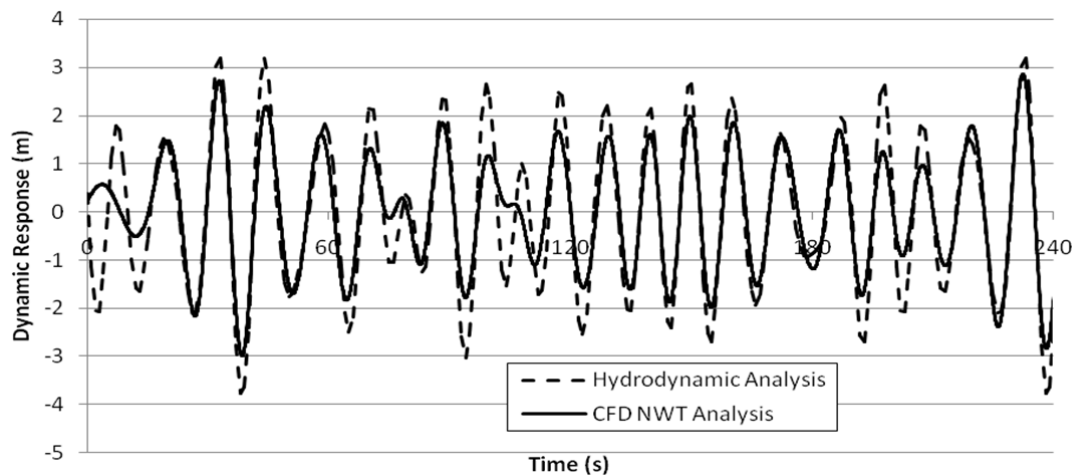


Fig. 7: Comparison of the dynamic response of the rectangular prism from the CFD NWT analysis and analytical hydrodynamic analysis

Discussions and conclusions

A numerical model suitable for aiding in the structural health monitoring (SHM) of wave energy converters (WECs) is presented. A numerical wave tank (NWT) is developed and is based on the methodology, which is described in a previous publication [9]. The model is validated by comparing the waves generated to those generated experimentally using the NUIG wave flume. The two outputs of wave elevation are compared in Fig. 2 at 2.35m and 6.75m from the inflow boundary and found to be in very good agreement.

The model is, then, extended in order to generate linear irregular waves, which can be used to model real ocean waves. The detailed methodology for generating linear irregular waves has been used to replicate a wave record observed at AMETS. A comparison between the analytical approximation of the measured wave and the output from the CFD model can be seen in Fig. 4. Since the model starts from a steady state, there is no correlation between the two waves in the initial stages of the simulation. However, after this stage, the two waves are found to be in very

good agreement in terms of both frequency and amplitudes. It is also observed that the CFD model tends to smoothen out any dramatic changes in the elevation. In other words, it tends to replicate low frequency, high amplitude waves better than high frequency, low amplitude waves.

A rectangular floating prism is then introduced into the model in order to explore the accuracy of wave-structure interaction prediction. A comparison of the dynamic response of the structure from the NWT model and the analytical solution, given in Eq. (5), is shown in Fig. 7. The two solutions were found to be in good agreement. The two solutions match very well in terms of frequency but there is a difference in the amplitude of the response. This may be attributed to; in the NWT model the structure is restricted to heave, or vertical, motion only while in the hydrodynamic analysis, all degree of freedom are accounted for. There is a large discrepancy in the initial part of the simulation between the two solutions, since the NWT model starts at a steady state. However, the two solutions begin to converge for the second half of the record.

References

- [1] S.H. Salter, Wave power. *Nature*. 249(5459) (1974) 720-724.
- [2] P.C. Chang, A. Flatau, S.C. Liu, Review Paper: Health Monitoring of Civil Infrastructure. *Structural Health Monitoring*. 2(3) (2003) 257-267.
- [3] H.Y. Guo, L. Zhang, L.L. Zhang, J.X. Zhou, Optimal placement of sensors for structural health monitoring using improved genetic algorithms. *Smart Materials and Structures*. 13(3) (2004) 528.
- [4] J. Goggins, B.M. Broderick, B. Basu, A.Y. Elghazouli, Investigation of the seismic response of braced frames using wavelet analysis. *Structural Control and Health Monitoring*. 14(4) (2007) 627-648.
- [5] J.M.W. Brownjohn, Structural health monitoring of civil infrastructure. *Philosophical Transactions of the Royal Society A: Mathematical, Physical and Engineering Sciences*. 365(1851) (2007) 589-622.
- [6] J.M. Nichols, . Structural health monitoring of offshore structures using ambient excitation. *Applied Ocean Research*. 25(3) (2003) 101-114.
- [7] L. Murawski, S. Opoka, W. Ostachowitz, *Measurement and calculation errors estimation and damage detection possibility analysis for SHM of offshore structure*, in *5th European Conference on Structural Health Monitoring, 2010*. 2010.
- [8] ANSYS-Inc., *ANSYS CFX, Release 12.1*. 2009.
- [9] W. Finnegan, J. Goggins, Numerical simulation of linear water waves and wave-structure interaction. *Ocean Engineering*. 43(0) (2012) 23-31.
- [10] ANSYS-Inc., *ANSYS AQWA, Release 13*. 2010.
- [11] Marine-Institute. *Marine Institute*. 2012 29-11-2012]; Available from: www.marine.ie.
- [12] A. Lal, M. Elangovan, CFD Simulation and Validation of Flap Type Wave-Maker. *World Academy of Science, Engineering and Technology*. 46 (2008) 7.
- [13] X.-f. Liang, J.-m. Yang, J. Li, L.-f. Xiao, X. Li, Numerical Simulation of Irregular Wave-Simulating Irregular Wave Train. *Journal of Hydrodynamics, Ser. B*. 22(4) (2010) 537-545.
- [14] M. Elangovan, Simulation of Irregular Waves by CFD. *World Academy of Science, Engineering and Technology* 55 (2011).
- [15] Y.-p. Zhao, T.-j. Xu, G.-h. Dong, Y.-c. Li, Numerical simulation of a submerged gravity cage with the frame anchor system in irregular waves. *Journal of Hydrodynamics, Ser. B*. 22(5, Supplement 1) (2010) 433-437.
- [16] G.-H. Dong, T.-J. Xu, Y.-P. Zhao, Y.-C. Li, F.-K. Gui, Numerical simulation of hydrodynamic behavior of gravity cage in irregular waves. *Aquacultural Engineering*. 42(2) (2010) 90-101.
- [17] T.-J. Xu, G.-H. Dong, Y.-P. Zhao, Y.-C. Li, F.-K. Gui, Analysis of hydrodynamic behaviors of gravity net cage in irregular waves. *Ocean Engineering*. 38(13) (2011) 1545-1554.
- [18] Coastal Engineering Research Center, *Shore protection manual / U.S. Army Coastal Engineering Research Center*, 1977. Fort Belvoir, Va. Washington: Supt. of Docs., U.S. Govt. Print. Off.

Citation: Finnegan W. and Goggins J. (2013). Numerical modelling to aid in the structural health monitoring of wave energy converters. Key Engineering Materials. 569-570: p. 595-602.

DOI: 10.4028/www.scientific.net/KEM.569-570.595 <http://www.scientific.net/KEM.569-570.595>